METALLIC SURFACES UNDER INTERPLANETARY MEDIUM – DEGRADATION MECHANISMS AND PROTECTION POSSIBILITIES

Maciej Sznajder [1,2], Ulrich Geppert [1,3]

[1] DLR Institute of Space Systems, Robert-Hooke-Straße 7, 28359 Bremen, Germany, +49 421 24420-1623, Maciej.Sznajder@dlr.de
[2]Institute of Physics, University of Zielona Góra, Szafrana 4a, 65-069 Zielona Góra, Poland
[3]Janusz Gil Institute of Astronomy, University of Zielona Góra, Lubuska 2, 65-265 Zielona Góra, Poland

ABSTRACT

Thin metallic films are commonly used in space industry. Important applications are e.g. multilayer insulation blankets (MLI) or solar sail membranes. In a sufficiently large distance from the Earth atmosphere, the solar wind and electromagnetic radiation are the dominating factors for material degradation. The solar protons while penetrating the metals recombine to neutral hydrogen atoms and then form molecular hydrogen bubbles. Their high concentration within the metals' lattice has a direct influence on their physical properties.

Up to now, no material that was exposed to the interplanetary space conditions has been returned to Earth. Therefore, studies both theoretical and experimental carried out in the terrestrial laboratories are necessary to predict the changes in the mechanical and thermo-optical properties of the metals.

The aim is to present the basics behind formation processes of molecular hydrogen bubbles as well as their influence on physical properties of exposed metals to the solar wind. The other degradation mechanisms are discussed as well, e.g. the delamination processes caused by corpuscular radiation. Ideas of protection possibilities of the metals are drawn.

The experimental studies were performed by use of the Complex Irradiation Facility (CIF) of the DLR's Institute of Space Systems in Bremen, Germany. The CIF's linear proton accelerator allows to irradiate specimens to well defined proton fluxes. A series of experiments have been made to simulate the growth of the bubbles at different physical conditions which represent those at the interplanetary space.

The post-degradation studies of the exposed metallic films have been performed by use of an electron microscope and number of image-processing methods to analyze the morphology of the specimens. It has been proven that at the early stage of the bubble growth the average bubble radius R evolves according to $R \sim t^{1/3}$ law.

One of the consequences of the molecular hydrogen bubbles formation is a significant increase of the metallic surface roughness or changes of the samples' thermo-optical properties. However, the bubble formation depends strictly on physical conditions at which the samples are exposed to the solar wind protons. Dependency on bubble formation mechanism due to temperature as well as proton kinetic energy is given.

1. INTRODUCTION

Thin metallic films made of vacuum deposited Aluminum layers on thin polyimide substrates are commonly used composite materials in space technology. Space environmental conditions cause

changes of their mechanical and thermo-optical properties. Therefore studies, both theoretical and experimental, allow to choose their properties, e.g. Aluminum thickness, which may well fit to a given space mission.
Here, one of the aging processes which take place in the interplanetary medium is presented: formation of molecular hydrogen bubbles onto metallic surfaces resulting from recombination processes of solar protons and the metal electrons.

Interplanetary medium is a dynamic environment which physical properties are determined by activity of the Sun. Therefore, experimental studies were focused on influence of the proton dose, the kinetic energy of the incident protons as well as the temperature of the specimens on formation of the molecular hydrogen bubbles.

The paper is organized as follows. In Section 2, the Complex Irradiation Facility is presented. Its linear proton accelerator was used to perform the experimental studies presented here. In Section 3, general principles and conditions for formation of the molecular hydrogen bubbles are given. In Section 4, the results from the experimental studies are presented. In Section 5, the conclusions are drawn.

2. COMPLEX IRRADIATION FACILITY

The Complex Irradiation Facility (CIF) was designed and commissioned with aim to perform material investigations under radiation conditions as prevalent in space environment. The complete facility has been built in UHV-technology with metal sealings. It is free of organic compounds to avoid self-contamination. The different pumping systems achieve a final pressure in the 10^{-10} mbar range (empty irradiation camber). The CIF advantage is that multiple radiation sources can be used at the same time, and therefore, specimens can be exposed simultaneous to both corpuscular- and electromagnetic- radiation. The facility is depicted in Fig. 1.

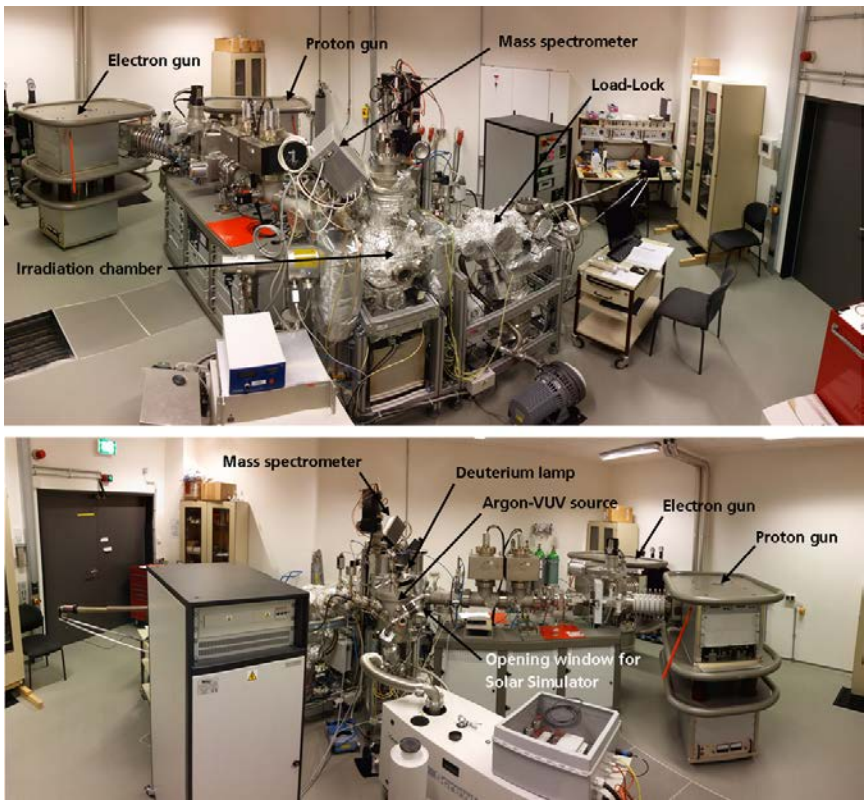

Fig. 1. The Complex Irradiation Facility at DLR, Bremen

The CIF is equipped with electron as well as proton linear accelerators. Kinetic energy of both projectiles can be set from a range of 1 keV to 100 keV. A minimum achievable current of both e^- and p^+ is 1 nA while the maximum one is 100 µA.

The protons are produced by ionization of hydrogen, which is stored in a lecture bottle inside the accelerator's deck. The hydrogen is guided through a thermo-mechanical gas inlet valve which remote control to the ion source. The ionization takes place inside the glass bulb of the source by excitation with radio frequency, which is capacitive coupled to the bulb. The plasma is confirmed and positioned by an axial permanent magnetic field [1].

The electrons are generated by a lanthanum hexaboride (LaB_6) cathode, which is a high performance, resistively heated, thermionic electron source. A heater current and Wehnelt voltage control the electron current [1].

Three electromagnetic sources are available, i.e. an Argon-VUV-source, a deuterium lamp and a Xenon-lamp (also called as the Solar Simulator, see Fig. 1). All three sources working simultaneously cover wide wavelength range from 40 nm to 2500 nm, see Fig. 2.

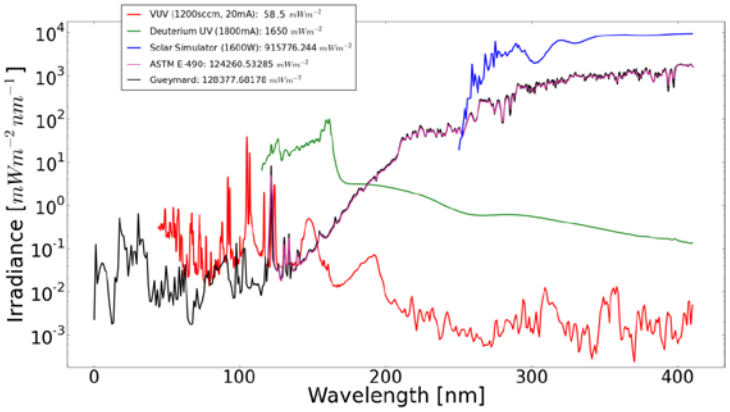

Fig. 2. The spectra of the CIF light sources compared to the solar radiation standards [2, 3].

3. FORMATION OF MOLECULAR HYDROGEN BUBBLES IN THE INTERPLANETARY SPACE

The degrading factors of the interplanetary space environment are the solar wind particles and the electromagnetic radiation. The solar wind is essentially made up of electrons and protons plus a small proportion of heavier ions, and it carries a magnetic field. Particles and fields are intimately coupled in plasmas [4]. Flux of solar protons and electrons taken from different databases is depicted in Fig. 3.

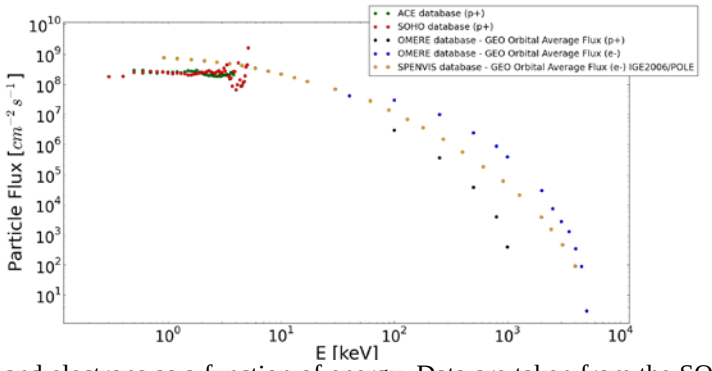

Fig. 3. Flux of solar protons and electrons as a function of energy. Data are taken from the SOHO, ACE, OMERE, and SPENVIS databases.

The molecular hydrogen bubbles are tiny (approx. 0.4 μm in diameter) metal pockets filled with molecular hydrogen gas. The H_2-gas is a result of recombination processes of the solar wind protons and electrons present within the metals. There are four recombination phenomenons of incident protons with electrons to the neutral hydrogen atoms: the Auger-, the resonant-, the Oppenheimer-Brinkman-Kramers-, and the Radiative Electron Capture- process. Since the solar wind consists mainly of low energetic protons (≤ 100 keV) the first three processes lead the recombination [5].

In the interplanetary space environment there are two requirements which need to be fulfilled to populate metallic surfaces with molecular hydrogen bubbles. First, is a minimum dose of protons necessary to initiate the bubble formation phenomenon. It has been verified experimentally that 10^{16} p^+ cm^{-2} are needed to observe bubble growth on Aluminum surfaces [6]. It is fulfilled in about few days (at 1 AU distance orbit from the Sun) considering the fact that a sample in the interplanetary space is permanently bombarded by a spectrum of the solar protons, see Fig. 3. Second is a temperature of a specimen exposed to the proton flux. The temperature needs to be high enough to start the bubble formation, but not too high to lose hydrogen much too rapidly due to the high diffusivity of hydrogen in metals. The temperature of a foil placed in a given distance *d* from the Sun can be calculated from the balance of heating and cooling by:

$$T = (0.5\ \alpha/\varepsilon\ 1SC/\sigma d^2)^{0.25}. \quad (1)$$

Here α is the solar absorptance, ε is the normal emittance, *SC* states for Solar Constant, σ is the Stefan-Boltzman constant. The thermo-optical parameters have been provided by the manufacturer of the Upilex-S foil, the UBE company. Solar absorptance and normal emittance are 0.093 and 0.017, respectively. The foil temperature as a function of a distance from the Sun is presented by solid black line, see Fig. 4.

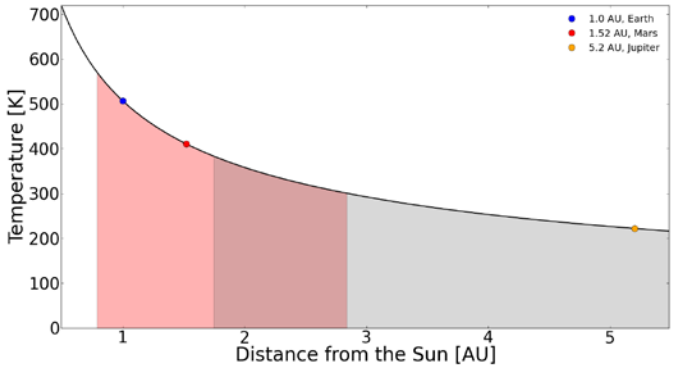

Fig. 4. Temperature of the foil as a function of the distance from the Sun.

The light-red area indicates orbits in the interplanetary space (Sun – sample distance given in AU) where samples temperature is too high to initiate the formation of the bubbles. The dark-red area shows an orbit range in which the bubble formation phenomenon has been confirmed by experimental studies performed at DLR. The grey area, i.e. for temperatures below ~300 K, indicates an orbit range which was not studied yet. The experimental findings are presented in Section 4.

4. HYDROGEN MOLECULAR BUBBLES ON VACUUM DEPOSITED ALUMINUM

A 7.5 μm thick Upilex-S foil covered both sides with vacuum deposited Aluminum (VDA) layer was used as a test material. Two thicknesses of the VDA coating were used, i.e. 100 nm and 1000

nm. The performed irradiation tests were devoted to justify environmental conditions for bubble formation. Different proton doses, kinetic energies of the incident ions, and temperatures of the specimens ware taken into the consideration. Therefore, three sets of irradiation experiments were performed.

The samples of set "A" were exposed to flux of 2.5 keV protons and each one with longer irradiation time, see Table 1, where t_S is a number of days in the interplanetary space until a probe will collect a given dose of protons. Results are shown in Fig. 5. From top to bottom, the pictures correspond to probes A1, A2, and A3, respectively. Average radii of bubbles have been estimated to 0.18 ± 0.05 μm, 0.19 ± 0.05 μm, and 0.2 ± 0.05 μm for probes A1, A2, and A3, respectively. There is a strict correlation between a dose of protons and the average bubble radius R for a given population. The bubbles grow according to $R \sim t^{1/3}$ law [5]. However, it must be pointed that the samples of set "A" have been exposed to relatively low proton doses, and therefore, more extended irradiation experiments are mandatory. Examining the electron microscope pictures, the surface density of bubbles has been estimated to ~10^8 cm^{-2}.

Table 1 Test parameters of probes set A, B, and C.

Probe symbol	**T [K]**	**E [keV]**	**D [p^+ cm^{-2}]**	**t_S [days]**	**t_{lab} [days]**	**t_S/t_{lab}**
A1	323	2.5	7.8 x 10^{17}	4.8	7.9	0.6
A2	323	2.5	8.2 x 10^{17}	5.0	5.5	0.9
A3	323	2.5	1.3 x 10^{18}	7.9	10.9	0.7
B1	300	2.5	4.3 x 10^{17}	3.6	5.1	0.7
B2	300	6.0	5.9 x 10^{17}	4.9	1.8	2.7
C1	338	10.0	2.65 x 10^{18}	13.4	1.9	7.0
C2	358	10.0	2.65 x 10^{18}	10.7	3.9	2.7
C3	383	10.0	2.65 x 10^{18}	8.2	1.9	4.3

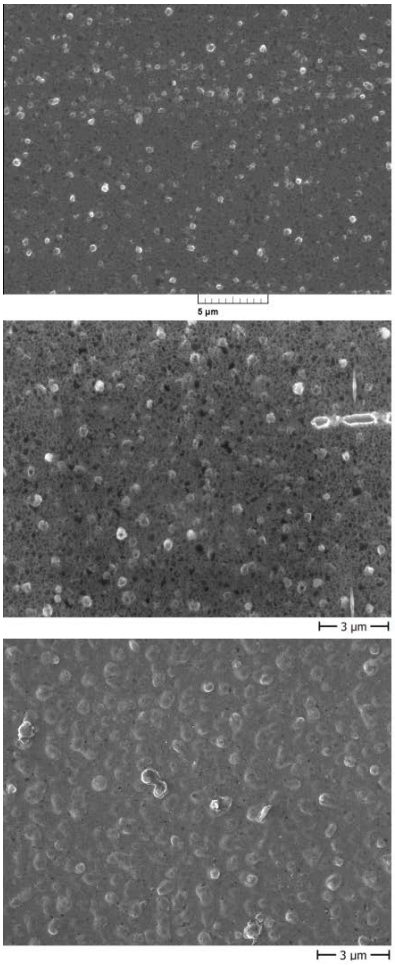

Fig. 5. Electron microscope pictures of probes A1 (top), A2 (middle), and A3 (bottom).

Samples of set “B” were exposed at room temperature to flux of protons with two different energies: 2.5 keV – sample B1 and 6.0 keV – sample B2. Probe B2 was irradiated slightly longer to the proton flux than probe B1, which has a direct influence on collected proton dose. Morphological studies of both specimens were made by use of an electron microscope. Results are shown in Fig. 6. Clearly, only the sample B1 was populated by the bubbles. Sample B2 does not exhibit the bubble formation phenomenon. Small dark points seen on the picture are the so-called delamination centers – small holes crated during the irradiation. Fig. 7 depicts penetration depths for 2.5 keV protons (left plot) and 6.0 keV protons (right plot) for Aluminum-Upilex-S film. For 2.5 keV protons 99.7% stuck within the Aluminum layer at an average depth of 34 nm and then form molecular hydrogen bubbles. For 6.0 keV protons only 67% stuck within the Aluminum at an average depth of 77 nm - rest is deposited within the Upilex-S structure. The protons break bonds of the Upilex-S molecules (polyimide molecules) and as a result a gas consisting of H_2, N_2, and O_2 gather between both layers, i.e. Aluminum and Upilex-S. When pressure of the gas is high enough the Aluminum breaks, release the gas and leave the Upilex-S substrate uncoated. That process is a radiation simulated delamination effect of Aluminum-Upilex-S film.

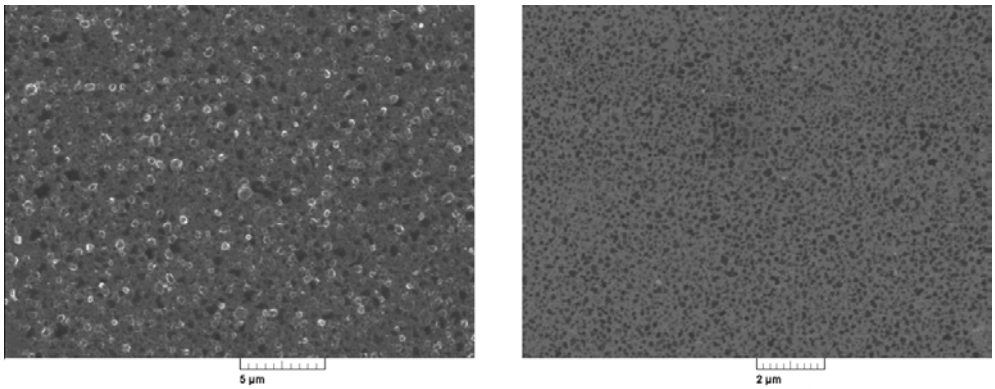

Fig. 6. Electron microscope pictures of probes B1 (left) and B2 (right).

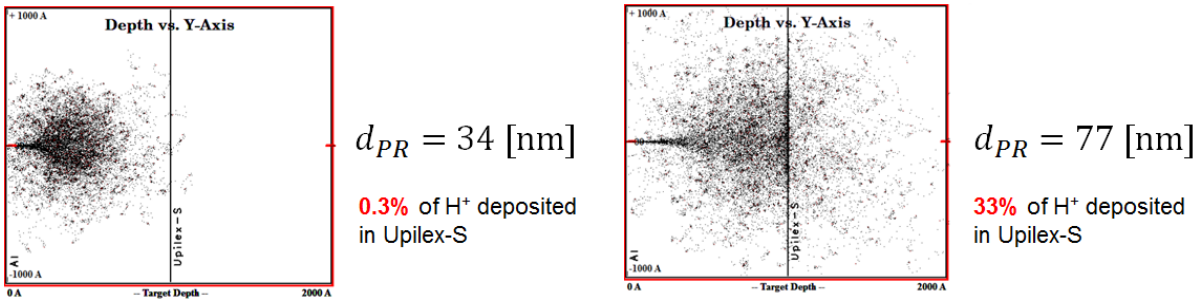

Fig. 7. Penetration depths for 2.5 keV and 6.0 keV protons penetrating Aluminum-Upilex-S film - sample B1 (left) and sample B2 (right).

The last set of samples, set “C”, was devoted to verify a boundary temperature at which formation of molecular hydrogen bubbles no longer proceeds. For such temperature all of the recombined hydrogen would diffuse out of the sample, and therefore, no bubble formation is possible. Three samples C1, C2, and C3 were exposed to flux of 10 keV protons at the temperature of 338 K, 358 K, and 383 K, respectively. 10 keV protons were chosen due to the fact that the linear proton accelerator of the CIF provides proton currents ≥ 0.1 µA for proton energies ≥ 10 keV. Such choice has significantly reduced the irradiation time of the specimens. For the irradiation test a thickness of 1000 nm VDA coating was used, since 10 keV protons would pass through the thin 100 nm coating, and therefore, no recombination and no bubble formation would take place.

Irradiation of the probe C1 at the temperature of 338 K brought an unexpected result. Few bubbles with diameter larger than 400 µm appeared on the surface see Fig. 8 (left column pictures). The

bubbles may grow to such dimensions due to the fact that the ratio of the proton flux used during the experiment and its equivalent in space f_{lab}/f_S was equal to 7.0. The increase number of incoming protons may accelerate the bubble growth in the lattice places where the non-Aluminum atoms/molecules are present. To check rather the flux is responsible for such effect, it may be worth to irradiate the sample with configuration of $f_{lab}/f_S = 1.0$.

Exposure of the probe C2 to the flux of protons at 358 K brought an important experimental result. The formed bubbles grown mainly on micro-scratches present on the foil's surface see Fig. 8 (middle column pictures).

Probe C3 was exposed to the proton flux at the highest considered temperature of 383 K. The probe was not populated by the bubbles. The temperature is a boundary parameter for the bubble formation mechanism. For comparison an un-irradiated sample is presented in the lower right picture.

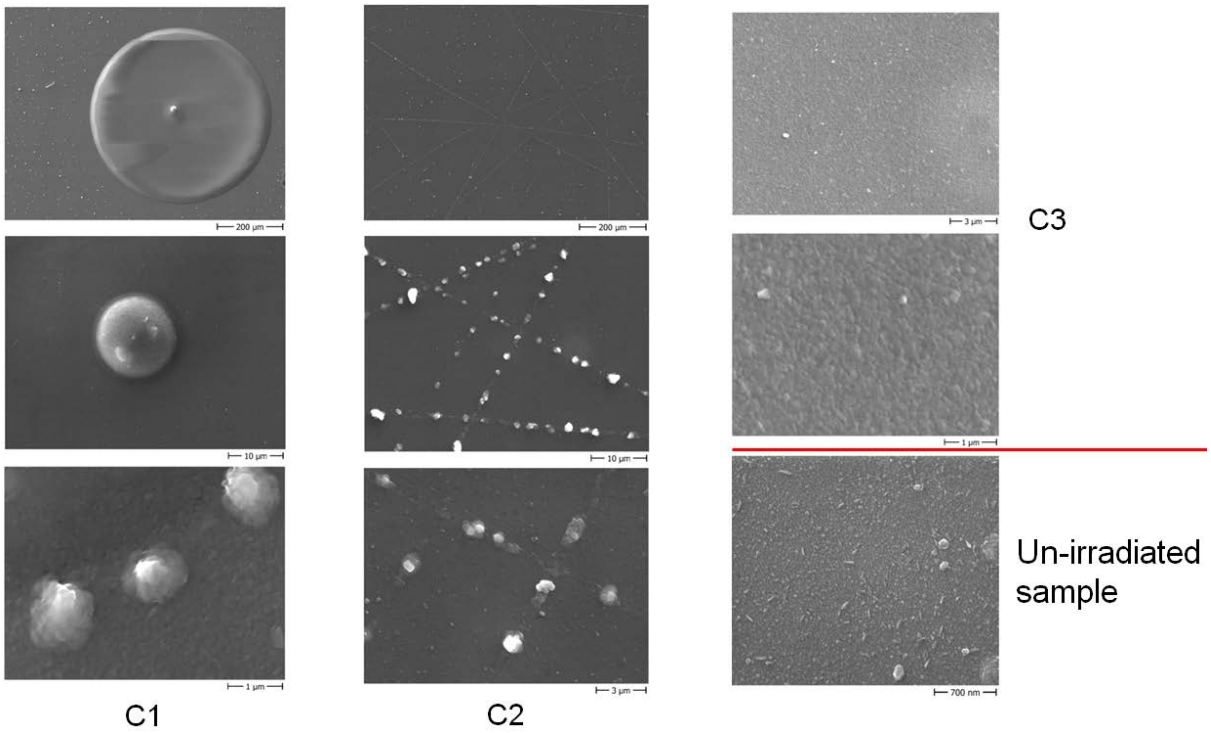

Fig. 8 Electron microscope pictures of samples: C1 (left), C2 (middle), C3 (upper right), and un-irradiated sample (lower right)

Protection possibilities of the metallic films against formation of the molecular hydrogen bubbles

Recombination of the solar protons and the metal electrons to the neutral hydrogen atoms is a precondition for formation of the molecular hydrogen bubbles. There are two possibilities to prevent the bubble formation.

First, is to keep the specimen at the temperature higher than 383 K. As proven in Section 4, at that temperature the recombined hydrogen atoms simply diffuse out from the sample and no bubble formation is possible.

Second, is to protect the metallic surfaces with protection coatings, e.g. made of transparent to visible light SiO_x or TiO_x. With such protection the incident protons would stuck within the layers structure, and therefore, would not reach the metallic substrate. Hence, no recombination and no bubble formation would take place.

5. CONCLUSIONS

Influence of the proton dose on bubble formation mechanism has been studied. Three samples have been exposed to 2.5 keV protons at the temperature of 323 K. It has been proven that the higher the proton dose, the larger the observed bubbles. Additionally it has been confirmed that the bubbles grow according to $R \sim t^{1/3}$ law [5].

The bubble formation mechanism as a function of proton kinetic energy has been investigated. It has been proven that the flux of 6.0 keV protons does not initiate the bubble growth mechanism (for the dose of 5.9×10^{17} p^+ cm^{-2} and thickness of the Aluminum layer of $\leq$ 100 nm) as opposed to lower energy protons. For that energy, 67% of the protons stuck in the Aluminum layer at the average depth of 77 nm. Rests of the protons degrade the Upilex-S structure. To produce the bubbles at the surface of the specimens, the larger proton doses are required.

Temperature influence on the bubble growth mechanism has been examined. It has been proven that the bubbles populate the VDA layers when the irradiated specimens' temperature varies from 300 K to 383 K. For the considered foils, that temperature range corresponds to the distance of 1.75 AU to 2.85 AU from the Sun. For the higher temperatures the hydrogen atoms diffuse from the sample out and no bubble formation is possible.

Experimental results pointed an interesting behavior of the bubble growth mechanism. Bubbles agglomerate on micro-scratches present on the Aluminum surface. It is an important result in context of the solar sail technology. Before the foil's deployment it is many times folded and rolled. Therefore, bubbles may gather in the places where such folds are present.

Future experimental studies will concern protection possibilities of the thin VDA coatings against destructing behavior of the solar protons. Two thin layers have been selected up to now, i.e. the SiO_x and the TiO_x with thicknesses which prevent the protons to penetrate and recombine to neutral hydrogen atoms within the Aluminum structure.

6. REFERENCES

[1] Renger T. and Sznajder M. and Witzke A. and Geppert U., *The Complex Irradiation Facility at DLR-Bremen*, Journal of Materials Science and Engineering A, Vol. 4, 1-10, 2014.

[2] ASTM, E490-00a, Solar Constant and Zero Air Mass Solar Spectra Irradiance Tables, reapproved 2006.

[3] Gueymard C.A., *The sun's total and spectral irradiance for solar energy applications and solar radiation models*, Solar Energy, Vol. 76, 423-453, 2004.

[4] Meyer N.V., *Basics of the Solar Wind*, Cambridge University Press, United Kingdom, 2007.

[5] Sznajder M. and Geppert U. and Dudek M., *Degradation of metallic surfaces under space conditions, with particular emphasis on Hydrogen recombination processes*, Advances in Space Research, Vol. 56, 71-84, 2015.

[6] Milacek L.H. and Daniels R.D. and Cooley J.A., *Proton radiation induced blistering of aluminum*, Journal of Applied Physics, Vol. 39, 2803-2815, 1968.